Aeroacoustic measurements of a deep cavity in a low speed flow

M. B. Jones[1], J. H. Watmuff[2] and S. M. Henbest[1]

[1]Air Vehicles Division, Defence Science and Technology Organisation, Melbourne, Victoria, 3207 Australia
[2] School of Aerospace, Mechanical and Manufacturing Engineering, RMIT University, Bundoora, Victoria, 3083 Australia

Abstract

Experimental results for the flow over a deep cavity in a low speed flow are reported. Fluctuating pressures were measured on the walls of a cavity model and beneath the upstream and downstream boundary layers. Based on these results a normal cavity tone was observed across the range of speed investigated. Hot-wire measurement of the streamwise velocity component were made in the shear layer and upstream boundary layer. However the velocity spectrums were broadband in nature which indicated that the cavity pressure tone is not due to an aeroacoustic resonance. Instead the pressure tone is due to a fundamental acoustic mode, where energy is extracted from the shear layer without feedback.

Introduction

Figure 1 shows the important flow features of a cavity flow and they are: boundary layer development upstream of cavity; separation and vortex shedding from upstream corner of cavity; shear layer above cavity; separated and possibly reattaching flow within the cavity; acoustic waves generated at downstream corner of cavity and acoustic waves generated due to elastic deflections of cavity walls.

The complexity of the flow stems from the coupling of the above aerodynamic and acoustic features. Under certain circumstances feedback loops can be established resulting in cavity resonance. The resonance can excite internal acoustic pressure levels of up to 170 dB. On aircraft, these high-intensity acoustic tones may lead to noise radiation, excessive heat transfer, structural fatigue, and interference with on-board avionic systems.

Predicting and understanding the aeroacoustic phenomena associated with cavity flows is important from a practical point of view. For example cavity type geometries exist on the external surfaces of aircraft in the form of: landing-gear wells, weapon bays, fuel vent recesses and instrumentation recesses. Aeroacoustic resonance can also occur in the presence of slots and gaps and such resonance is often referred to as an *edge tone*.

Due to the complex interaction of the flow and acoustic fields, accurate analytical or numerical prediction of the frequency and amplitude of the cavity tone(s) is difficult. However, the simple vortex-acoustic feedback model of Rossiter [10] provides reasonable prediction of the resonant frequencies across a limited range of Mach numbers and cavity geometries. The Rossiter model predicts resonant frequencies

$$St = \frac{fL}{U_\infty} = \frac{m-\gamma}{M+1/K},\qquad(1)$$

where f is the frequency of the pressure fluctuations, L is the cavity length, m is an integer representing the mode, γ is a phase lag, M is the freestream Mach number, K is an empirical constant that corresponds to the average vortex convection velocity divided by the freestream velocity, U_∞, and St is the non-dimensional frequency (otherwise known as the Strouhal number).
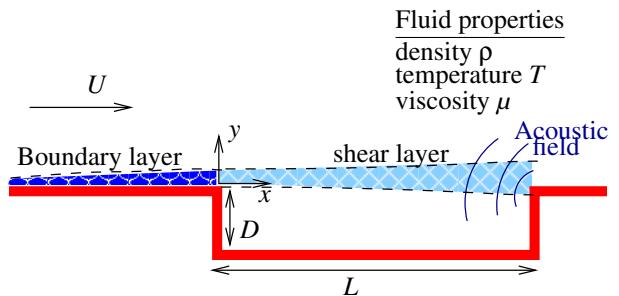

Figure 1: Cavity flow features.

Recently the authors have carried out a literature review of the existing data, as well as empirically based and analytical based prediction methods. Based on the literature reviews ([16], [7]) the following conclusions are summarised: the conditions leading to cavity resonance are not well defined; the number of relevant parameters influencing cavity resonance may be large (e.g. cavity geometry, upstream influence, Mach number, Reynolds number etc.); analytical and semi-empirical methods for predicting the frequency of the tones perform reasonably well across certain Mach number ranges; however, these methods can not predict the intensity of the tones or indeed whether the tones will appear at all; and there is little published flight-test data (full scale data); hence, the accuracy of scaling wind tunnel data to flight conditions remains unclear. To address this, systematic experiments are planned across a range of Mach numbers, cavity geometries and length scales (e.g. upstream boundary layer thickness relative to cavity scale). Preliminary experimental results for a low speed flow have been obtained and are presented in this paper.

Experimental Method

Experiments were performed in the Research Wind Tunnel (RWT) at DSTO. This is a suction tunnel and has a maximum freestream velocity of 30 m/s. The inlet has an octagonal cross section incorporating a bell mouth followed by the settling chamber which contains two screens. A 4:1 contraction accelerates the flow into the working section which has an octagonal cross section with a maximum width of 0.8 m a maximum height of 0.62 m and a length of 1.20 m. The working section was found to have a freestream turbulence intensity of $\sqrt{\overline{u'^2}}/U_\infty < 0.5\%$, where u' is the fluctuating velocity component in the streamwise direction and on over-bar denotes an averaged value.

Experimental Model

The cavity had fixed dimensions of: length, $L = 50$ mm, depth, $D = 100$ mm and width, $W = 300$ mm. The cavity model was incorporated into the floor of the working section. The front corner of the cavity was located approximately 100 mm from the exit of the contraction. The coordinate system is shown in figure 2 and the origin of the coordinate system is located on the upstream corner of the cavity at the cavity mid-span.
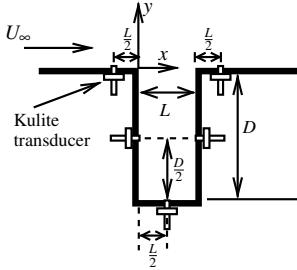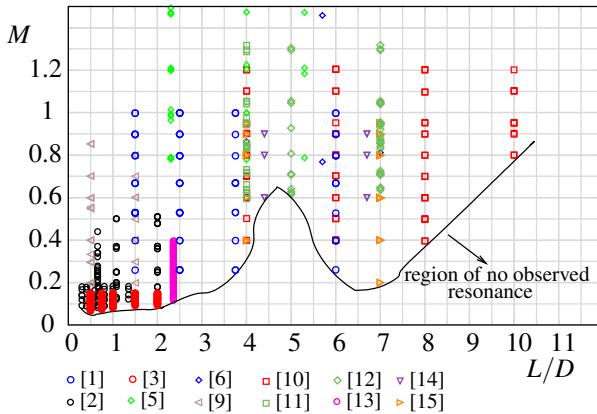
Figure 2: Kulite locations.

Figure 3: Observed resonance for $M < 1.5$.

Justification for choosing $L/D = 1/2$

Based on the velocity range of the RWT, and the limitation on model scale, it was known that strong intensity tones were unlikely to be observed. Nevertheless the model was designed to produce resonant tones. Figure 3 shows the Mach number and L/D ratio for the data reviewed in [7] and re-analysed here, for which resonant tones were reported. Referring to figure 3, most of the low speed data where resonance has been observed occurs for $L/D \lesssim 2.5$. Here low speed refers to a Mach number less than 0.2. It should be kept in mind that the analyses of existing data was not exhaustive, further the lack of resonant data at low speeds for $L/D \gtrsim 2.5$ may simply reflect the fact that experiments have not been reported in this range. Of the data presented in figure 3, the data of [3] is at the lowest velocities, with resonance reported down to $M = 0.068$ (23.6 m/s). The data of [3] covers the range $0.5 \leq L/D \leq 2.0$ and the lowest velocity at which resonance occurred was for an $L/D = 0.5$. Hence, the ratio $L/D = 0.5$ was chosen to increase the probability of resonance being observed.

Pressure transducers

Fluctuating pressures were measured along the x axis at locations: upstream of the cavity, on the front wall of the cavity, on the floor of the cavity, on the rear wall of the cavity and downstream of the cavity, figure 2. Pressure measurement were made at freestream velocities $U_\infty = 16, 20, 25$ m/s. The fluctuating pressures were measured using *Kulite Semiconductor* model XT-140m-25A pressure transducers where the suffix 25A indicates the transducers are rated to 25 PSI and measure absolute pressure. The transducers have a linear response with a nominal full scale output of 100 mV.

Hotwire anemometry

Using hotwire anemometry, the x-component of velocity, $U(t)$,

was measured at 5 streamwise stations across the shear layer ($x/L = 0.02, 0.25, 0.5, 0.75$ and 0.9) and at 1 location in the upstream boundary layer ($x/L = -1.4$). The single hotwire probe (Dantec P055) had a prong tip separation of approximately 3 mm. The hot-wire filament was made from Wollaston wire which had a platinum core diameter of 5 μm and an active length of 1 mm. A y-traverse was performed, starting at a location within the cavity and traversing out to the freestream. All hotwire measurements were performed at the fixed spanwise coordinate $z/L = 0$. Hotwire measurements were only performed for the $U_\infty = 20$ m/s case.

Data acquisition

The Kulite pressure transducer is a strain gauge device which is amplified using a *Dewetron* strain gauge amplifier before being sampled by a 24-bit data acquisition board, which can sample 16 channels simultaneously. The signals were sampled for a period of 180 s, at a sampling rate of 5 kHz. The strain gauge amplifier also provides filtering capabilities and the filters were set to low pass *Butterworth* type with a cut off frequency of 2.5 kHz. Prior to taking a measurement an offset amplifier gain was applied to the output of all the pressure transducers such that zero volts output corresponded to atmospheric pressure. This was equivalent to setting the transducers to measure *gauge* pressure and all the data logged is then relative to atmosphere.

The output from the hot-wire anemometer was passed through a low pass filter with the cutoff frequency set to 5 kHz. The filtered hot-wire signal was then sampled using a National Instruments USB data acquisition module (model USB-9215A). The sample rate for all hotwire measurements was 10 kHz and the total sample time was 90 s for each coordinate.

Fluctuating pressure results

The dimensional power spectral density of pressure fluctuations, Φ'_p, for the boundary layer and cavity pressure transducers is plotted in figure 4 for the $U_\infty = 25$ m/s case only and clear spectral peaks are evident. The dominant peaks were found to correspond to the fundamental blade passing frequency, f_{bp_1}, and its harmonics (f_{bp_2}, f_{bp_3} etc.). The fundamental blade passing frequency is given by $f_{bp_1} = N \times f_{\text{fan}}$, where $N = 24$ is the number of blades and f_{fan} is the fan rotational speed in Hz. The rotational speed of the fan was recorded allowing f_{bp_1} to be calculated for a given tunnel velocity and for the $U_\infty = 25$ m/s case the predicted values are marked in figure 4. A much weaker spectral peak (red circle in figure 4) is evident and is 2 orders of magnitude less than f_{bp_1}. This weaker spectral peak remains relatively fixed at ≈ 570 Hz across the limited range of velocities tested but increases in amplitude with increasing velocity.

The weak spectral peaks appear on the transducer signals measured within the cavity and to a lesser extent in the upstream and downstream boundary layer. However it is not apparent on the reference transducer mounted on the wind-tunnel wall (not shown) nor was it evident in measurements performed with the tunnel in a clean configuration. Therefore it is concluded that this spectral peak is associated with a cavity tone. Figure 5 shows how the intensity of this cavity tone varies in the streamwise direction for the range of freestream velocities measured. In figure 5 the data is presented in non-dimensional form where $\Phi_p = 4\Phi'_p/(\rho^2 U_\infty^3 L)$ and ρ is the fluid density. This cavity tone is not a Rossiter [10] tone since the frequency does not scale with freestream velocity, rather it is believed to be associated with the normal mode cavity tone, which is expected to scale with cavity depth and speed of sound [4].

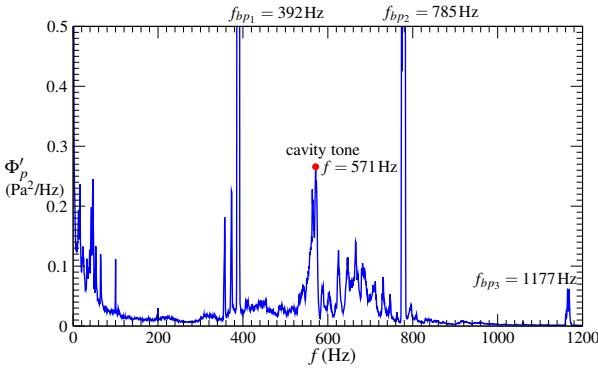A simple method for predicting the normal mode frequency is

Figure 4: Power spectral density of fluctuating pressures measured on the floor of the cavity for $U_\infty = 25$ m/s. A cavity normal mode tone occurs at $f = 571$ Hz. Fundamental blade passing frequency and harmonics are also evident (predicted values are marked).
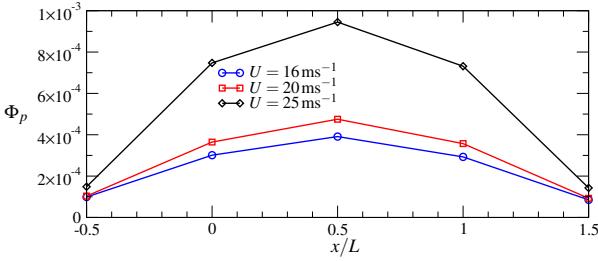

Figure 5: Nondimensional magnitude of the normal mode pressure tone as a function of x/L, for different freestream velocities.

given in [4], who finds that a curve fit of the form:

$$\frac{fD}{a} = \frac{0.25}{1 + A(L/D)^B}, \qquad L/D \lesssim 2 \qquad (2)$$

is a very close fit to the full solution given in [9], where a is the speed of sound and the constants have values of $A = 0.65$ and $B = 0.75$. Alternatively expressing (2) in terms of a lengthwise Strouhal number gives:

$$\frac{fL}{U_\infty} = \frac{0.25(L/D)}{M[1 + A(L/D)^B]}, \qquad L/D \lesssim 2. \qquad (3)$$

Equation (3) is plotted in figure 6 along with the results from the current study, also shown are experimental results from 3 separate studies which all had an L/D ratio of 0.5. For comparison the Rossiter modes as predicted by (1) are shown where the empirical constants $K = 0.57$ and $\gamma = 0.25$ have been used [10].

Shear layer velocity results

Mean streamwise velocity in shear layer

The mean streamwise velocity profiles measured in the shear layer and upstream boundary layer are plotted in non-dimensional form in figure 7, where the local freestream velocity, U_1, and cavity depth, D, have been used to normalise the profiles. Of note is the large mean velocity gradient which is exhibited by the $x/L = 0.02$ profile around $y = 0$. For the $x/L = 0.02$ profile the flow appears quiescent for coordinates $y \lesssim 0.2$ mm. The location of the outer edge of the shear layer was defined using a 99% of freestream velocity criterion. Using this definition the outer edge of the shear layer was found to
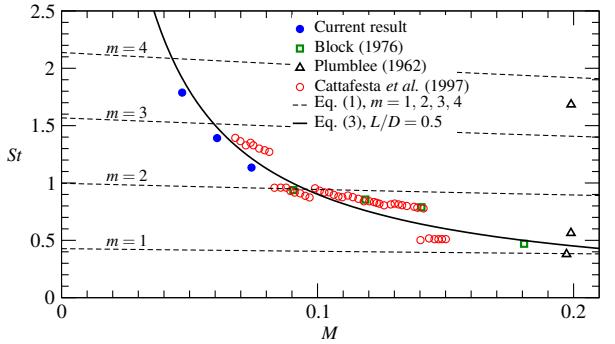

Figure 6: Nondimensional resonant frequencies as a function of Mach number, $L/D = 1/2$ for all the data shown.

grow from 15.1 mm at $x/L = 0.02$ to 19.8 mm at $x/L = 0.9$. Interference of the probe body with the downstream corner of the cavity made it difficult to measure within the cavity particularly for the downstream stations ($x/L = 0.75$ and $x/L = 0.9$) where it was not possible to traverse to the lower edge of the shear layer. However from the upstream corner of the cavity to $x/L = 0.5$ the lower edge of the shear layer grows by approximately 8 mm over a length of 25 mm.
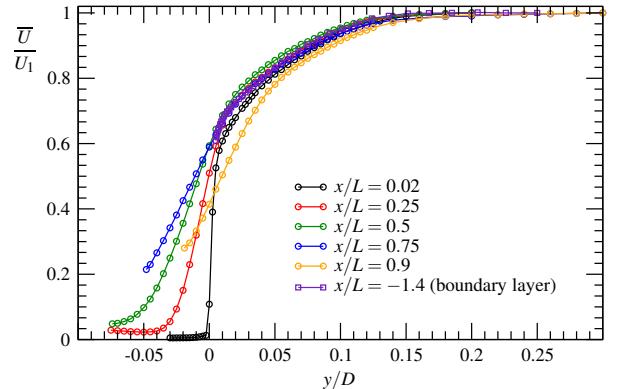

Figure 7: Mean streamwise velocity profile measured in the shear layer at different x/L locations for $U_\infty = 20$ m/s.

RMS of streamwise velocity fluctuations in shear layer

The RMS of streamwise velocity fluctuations is plotted in non-dimensional form in figure 8. There is a sharp increase in $\sqrt{\overline{u'^2}}$ across the $y = 0$ plane at the upstream station ($x/L = 0.02$). As was the case for the mean velocity profiles it is the shear layer within the cavity that exhibits the most significant changes as it develops in the streamwise direction. The RMS of streamwise velocity fluctuations in outer part of the shear layer ($y > 0$) shows little change with the streamwise direction and it is not until ($x/L = 0.9$) that a significant change in the profile occurs.

Power spectral density of velocity fluctuations

A representative PSD of the streamwise velocity fluctuations, measured within the shear layer and at location $x/L = 0.5$, is presented as a surface plot, $\Phi'_u(f, y)$, in figure 9. This method of presentation allows the data to be visually inspected for the presence of spectral peaks. However from inspection of figure 9 no significant tones are present in the streamwise velocity signal. The behaviour of the PSD at the other streamwise station is similar to figure 9, in that no spectral peaks are evident. The only exception is at the $x/L = 0.25$ station where spectral peaks
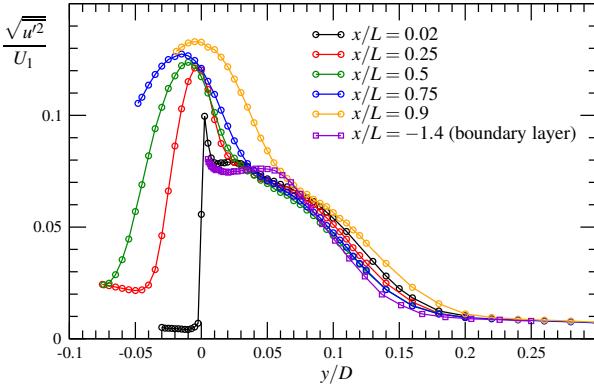
Figure 8: RMS of streamwise velocity fluctuations measured in the shear layer at different x/L locations for $U_\infty = 20$ m/s.
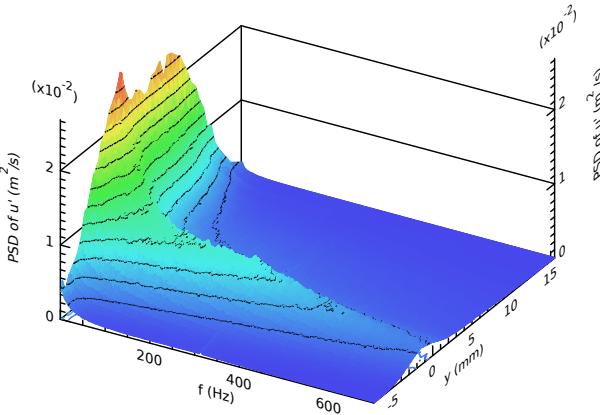

Figure 9: PSD of streamwise velocity at $x/L = 0.5$ for $U_\infty = 20$ m/s.

appear at $f = 312.6$ Hz and $f = 625.2$ Hz, which align with the predicted blade passing frequencies.

Conclusions

A cavity having a length to depth ratio of $1/2$ exhibited a spectral peak in the wall pressure signal measured within the cavity and in the upstream and downstream boundary layers. The frequency of the spectral peak was found to be fixed at $f \approx 570$ Hz across the freestream velocity range of the experiments (16-25 m/s). The spectral peak is believed to correspond to the cavity normal mode and the frequency is well predicted by the curve fit of [4]. The intensity of the cavity normal mode is weak in comparison to the background blade passing frequencies. However the background blade passing frequencies do not appear to interact or excite cavity modes and their effect can safely be ignored. The cavity normal mode does not appear to couple with the shear layer freestream velocity and therefore is not explained by the Rossiter [10] feedback model.

References

[1] Ahuja, K. K. and Mendoza, J., Effects of cavity dimensions, boundary layer, and temperature on cavity noise with emphasis on benchmark data to validate computational aeroacoustic codes, Contractor Report NASA-CR-4653, NASA, 1995.

[2] Block, P. J. W., Noise response of cavities of varying dimensions at subsonic speeds, Tech. Note NASA-TN-D-8351, NASA, 1976.

[3] Cattafesta III, L. N., Garg, S., Choudhari, M. and Li, F., Active control of flow-induced cavity resonance, Technical Report AIAA-1997-1804, AIAA, USA, 1997.

[4] East, L. F., Aerodynamically induced resonance in rectangular cavities, *Journal of Sound and Vibration*, **3**, 1966, 277–287.

[5] Heller, H. and Bliss, D., Aerodynamically induced pressure oscillations in cavities - physical mechanisms and suppression concepts, Technical report AFFDL-TR-74-133, Air Force Flight Dynamics Lab, USA, 1975.

[6] Heller, H. H., Holmes, D. G. and Covert, E. E., Flow-induced pressure oscillations in shallow cavities,, *Journal of Sound and Vibration*, **18**, 1971, 545–546.

[7] Jones, M. B. and Watmuff, J., Scaling of cavity-flow wind-tunnel data, in *Thirteenth Australian Aeronautical Conference*, 2009.

[8] Karamcheti, K., Acoustic radiation from two-dimensional rectangular cutouts in aerodynamic surfaces, NACA Technical Note NACA-TN-3487, NACA, 1955.

[9] Plumblee, H. E., Gibson, J. S. and Lassiter, L. W., A theoretical and experimental investigation of the acoustic response of cavities in an aerodynamic flow, Technical Report WADD TR-61-75, USAF, 1962.

[10] Rossiter, J. E., Wind-tunnel experiments on the flow over rectangular cavities at subsonic and transonic speeds., ARC Reports and Memoranda 3438, Aeronautical Research Council, 1964.

[11] Shaw, L. L., Smith, D. L., Talmadge, R. D. and Seely, D. E., Aero-acoustic environment of a rectangular cavity with a length to depth ratio of four, Technical report AFFDL-TR-74-19-FYA, Air Force Flight Dynamics Lab, USA, 1974.

[12] Smith, D. L., Shaw, L. L., Talmadge, R. D. and Seely, D. E., Aero-acoustic environment of rectangular cavities with length to depth ratios of five and seven, Technical report AFFDL-TR-74-79-FYA, Air Force Flight Dynamics Lab, USA, 1974.

[13] Tam, C. K. W. and Block, P. J. W., On the tones and pressure oscillations induced by flow over rectangular cavities, *Journal of Fluid Mechanics*, **89**, 1978, 373–399.

[14] Tracy, M. B. and Plentovich, E. B., Characterisation of cavity flow fields using pressure data obtained in the langley 0.3-meter transonic cryogenic tunnel., Tech. Rep. NASA-TM-4436, NASA Langley Research Center, 1993.

[15] Tracy, M. B. and Plentovich, E. B., Cavity unsteady-pressure measurements at subsonic and transonic speeds, NASA Technical paper 3669, NASA Langley Research Center, 1997.

[16] Watmuff, J. H., Review of cavity aeroacoustic phenomena and previous research initiatives, Technical Report, DSTO (To appear), 2010.